ANALYTICAL SCIENCES JANUARY 2020, VOL. 36

Ga Ion-doped ZrO_2 Catalyst Characterized by XRD, XAFS, and 2-Butanol Decomposition

Takashi YAMAMOTO*,† and Akihito KURIMOTO****

*Department of Natural Science, Faculty of Science and Technology, Tokushima University, Tokushima 770–8506, Japan

**Department of Mathematical and Material Sciences, Faculty of Integrated Arts and Sciences, Tokushima University, Tokushima 770–8502, Japan

Group 2, 3, and 13 element-doped zirconium oxide catalysts *M*-ZrO_2 (M = Mg, Sr, Y, La, Ce, Sm, Er, Yb, B, Al, Ga, In, and Tl; 5 mol%) were prepared by impregnation of each metal salt aqueous solution on amorphous zirconium hydroxide, followed by calcination at 773 K. The *M*-ZrO_2 samples were characterized by the catalytic performance of 2-butanol decomposition at 573 K, XRD, XANES and EXAFS spectroscopic techniques. Detailed analyses were performed herein for a series of Ga–ZrO_2 with various doping amounts in the range of 1 – 60 mol%. The addition of Group 2 and 3 elements little influenced the catalytic performance of ZrO_2 itself to promote dehydration to produce 1-butene with 90% selectivity. Ga–ZrO_2 and In–ZrO_2 gave methyl ethyl ketone as the main product *via* dehydrogenation. The doped Ga ion mainly existed inside the bulk of zirconia by forming the $Ga_xZr_{1-x}O_2$ solid solution up to 5 mol%. Highly doped species more than 10 mol% aggregated to form ε-Ga_2O_3. Each fraction forming the solid solution and Ga_2O_3-like species was evaluated by XANES analysis.

Keywords Ga_2O_3, ZrO_2, solid solution, catalyst, 2-butanol dehydrogenation, XANES, EXAFS, XRD

(Received August 22, 2019; Accepted September 26, 2019; Advance Publication Released Online by J-STAGE October 4, 2019)

Introduction

As for a heterogeneous catalyst, various kinds of ZrO_2 are known to possess both acid and base sites, and have been of considerable practical and fundamental interests because of their properties to promote several kinds of catalytic reactions, such as dehydration including α-olefin synthesis *via* the Hoffman elimination of secondary alcohol, hydrogenation, *iso*-butene, or methanol synthesis from a CO–H_2 mixture, the Tishchenko reaction, the Meerwein–Ponndorf–Verley (MPV) reduction, and so on.[1-6] It is well known that the addition of metal cations into ZrO_2 often generates valuable properties apart from both the component metal oxides themselves and/or drastically enhances their own specific properties. The oxygen storage capacity related to reduction behavior of lanthanoid elements in CeO_2–ZrO_2,[7,8] oxygen ion mobility for Sc_2O_3–, Y_2O_3– and Nd_2O_3–ZrO_2,[9-12] strong acidity for MoO_3–ZrO_2 and WO_3–ZrO_2,[13,14] and TiO_2–ZrO_2 solid solutions[15] are the examples. The development of novel ZrO_2-based functional materials and their improvement have been the subject of considerable investigations.

We have been investigating the catalytic performance of zirconium oxide-based binary oxide catalysts and their structure. A conventional active WO_x–ZrO_2 strong solid acid catalyst was proposed to consist of a WO_3–ZrO_2 solid solution, WO_6 aggregates (WO_x cluster), and isolated WO_4 species on the surface.[16,17] Our model structure is generally the same as that in the previous publications as for the existence of a small WO_3 cluster,[18,19] but has been modified by W K- and L1-edge X-ray absorption fine structure (XAFS) analysis and the use of a thermodynamic phase diagram. Using various kinds of tungsten oxide catalysts supported in Y-doped ZrO_2, we proposed the crystalline phase of tetragonal zirconia that plays the intrinsic role of generating a strong solid acidity, which relates to the stabilization of small WO_3 clusters without aggregation to a large particle.[20] Hydrothermally ill-crystalized binary oxides with a ZrW_2O_8 composition were recently confirmed to act as a strong solid acid.[21]

It is well known that alkaline earth oxides (Group 2 elements) and rare earth oxides (Group 3 elements) act as solid base catalysts, and the acid-base properties of an oxide in Group 13 elements are different for each element.[2,5,6] The addition of these elements to ZrO_2 might influence the catalytic performance of ZrO_2. In the present study, we prepared Group 2, 3, and 13 element-doped ZrO_2 by impregnation of metal salt onto amorphous zirconium hydroxide, followed by calcination. The surface properties were examined using 2-butanol conversion as a model catalytic reaction. The textural and local structures were also investigated by X-ray diffraction (XRD) and XAFS.

Experimental

$Zr(OH)_x$ was obtained by hydrolysis of $ZrOCl_2{\cdot}8H_2O$ (Nacalai Tesque, GR) with 25 mass% NH_3 aqueous solution at room temperature.[16,20] The final pH value was adjusted to 10, and the

† To whom correspondence should be addressed.
E-mail: takashi-yamamoto.ias@tokushima-u.ac.jp

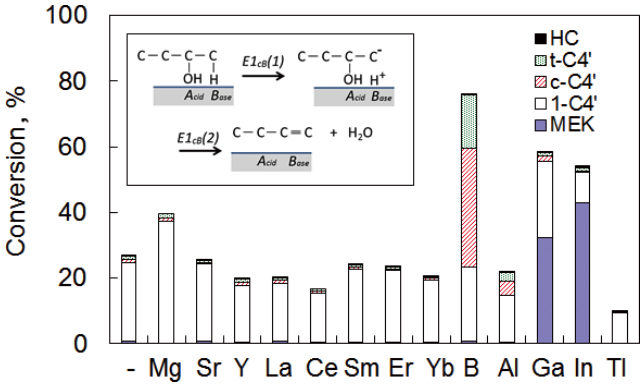

Fig. 1 Results of the 2-butanol decomposition over the metal ion-doped ZrO_2 catalysts at 573 K. Catalyst, 0.1 g; total flow rate, 20 mL/min; 2-butanol, 5%; N_2, balance; 1 atm. HC, Hydrocarbons (C1 – C3); *t*-C4′, *trans*-2-butene; c-C4′, *cis*-2-butene; 1-C4′, 1-butene; MEK, methyl ethyl ketone. The inset denotes possible mechanism of 1-butene formation *via* $E1_{cB}$ mechanism.

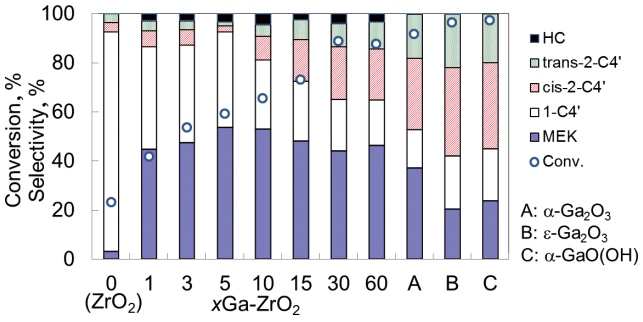

Fig. 2 Dependence of the doping amount of Ga on the 2-butanol decomposition over Ga–ZrO_2. Catalyst, 0.1 g; total flow rate, 20 mL/min; 2-butanol, 5%; N_2, balance; 1 atm. HC, Hydrocarbons; *t*-C4′, *trans*-2-butene; c-C4′, *cis*-2-butene; 1-C4′, 1-butene; MEK, methyl ethyl ketone.

aging time was 12 h. The obtained gel was repeatedly washed with distilled water until free of Cl^- by the $AgNO_3$ test, then dried at 383 K for 12 h. Metal-ion-doped zirconium oxides were prepared by impregnation of $Zr(OH)_x$ with an aqueous solution of metal salt at 353 K, followed by calcination at 773 K for 3 h in air. As for the metal salt, H_3BO_3, $Al(NO_3)_3{\cdot}9H_2O$, $Y(NO_3)_3{\cdot}nH_2O$, $In(NO_3)_3{\cdot}3H_2O$, $Ce(NO_3)_3{\cdot}6H_2O$, $Sm(NO_3)_3{\cdot}nH_2O$, $Yb(NO_3)_3{\cdot}nH_2O$, $TlNO_3$ (Wako Pure Chemical), $Mg(NO_3)_2{\cdot}6H_2O$, $La(NO_3)_3{\cdot}6H_2O$ (Nacalai), $Ga(NO_3)_3{\cdot}nH_2O$ (Kojundo Chemical Laboratory), $Sr(NO_3)_2$ (Kishida Chemical), and $Er(NO_3)_3{\cdot}nH_2O$ (Rare Metallic) were utilized. The prepared catalyst is denoted as *M*-ZrO_2 or *x*MZ, where *x* and *M* refer to the molar fraction of a metal atom to zirconium and a kind of doped element, respectively. Except for Ga, the amounts of doped element were 5 mol% based on a monomer molecule.

Gallium oxide and oxyhydride polymorphs were prepared with reference to a previous publication.[22,23] α-GaO(OH) was obtained by the hydrolysis of the gallium nitrate aqueous solution with the NH_3 aqueous solution at pH 9 and filtration, followed by drying at 383 K for 12 h. α-Ga_2O_3 was obtained by calcination of α-GaO(OH) at 773 K for 3 h in air. The β- and ε-Ga_2O_3 were obtained by calcination of gallium nitrate in air for 3 h at 1073 and 773 K, respectively.

XRD patterns were recorded with a Miniflex diffractometer (Rigaku) equipped with a Ni-filtered Cu Kα radiation source.

Ga K-edge X-ray absorption spectra were recorded with a Looper (Rigaku) laboratory-type spectrometer[24] in transmission mode at room temperature. An open-type X-ray tube equipped with a LaB_6 filament and a Mo cathode, an Ar-gas sealed proportional counter, and a scintillation counter were used as the X-ray source and detectors for incident and transmitted X-rays, respectively. The X-ray tube was set to 22 kV – 50 mA. The Si(620) and Si(400) monochromator crystals were used for the X-ray absorption near edge structure (XANES) and extended X-ray absorption fine structure (EXAFS) experiments, respectively. Energy was not calibrated. Data reduction for the EXAFS analysis was performed with the REX2000 program.[25] For the XANES, background removal and normalization of the spectra were performed using the Igor Pro 6.2 program[26] according to the procedure reported by Tanaka *et al.*[27] A quantitative component analysis for the XANES spectra by a least-squares method was also performed with Microsoft Excel 2010. The phase shift and backscattering amplitudes were calculated using the FEFF8.4 program.[28]

The BET specific surface area was calculated by an analysis of the N_2 adsorption isotherm recorded with a BELSORP-mini (MicrotracBEL) at 77 K. Each sample was outgassed at 573 K for 2 h prior to the measurement.

The 2-butanol decomposition was performed in a fixed-bed reactor at an atmospheric pressure and at 573 K. The total flow rate was 20 mL/min, and the 2-butanol concentration was 5 vol% with N_2 as the balance. Prior to the reaction, 100 mg of each catalyst sample was treated at 673 K for 2 h under 50 mL of N_2 stream. The product distributions were analyzed using a GC-8A gas chromatograph (Shimadzu Corp., Japan) equipped with a flame ionization detector.

Results

Catalytic activity of 2-butanol conversion

Figure 1 shows the results of the 2-butanol decomposition over the metal ion-doped zirconia. ZrO_2 itself produced 1-butene with 90% selectivity, and the addition of alkaline earth metals (Mg and Sr) and rare earth elements (Y, La, Ce, Sm, Er, and Yb) little affected both the activity and product distributions. In the case of the Group 13 elements, the addition of B, Ga, and In improved the activities of the 2-butanol conversion by *ca.* three times. The 2-butene formation was mainly promoted by B–ZrO_2. The dehydrogenation reaction to form methyl ethyl ketone (MEK) preferentially proceeded over Ga- and In-doped ZrO_2.

It has been reported that gallium oxide itself and the supported species were hardly reduced by hydrogen below 773 K (less than 2%)[29–31] whereas supported In species were reduced in some parts below 600 K.[32,33] Lower alcohol sometimes acts as a reducing agent even at a mild condition. Then effects of the doping amount on the catalysis for the 2-butanol decomposition for the Ga–ZrO_2 catalysts were examined. Figure 2 summarizes the conversion and product distributions (selectivities) by Ga–ZrO_2 with different doping amounts. The results for the three kinds of gallium oxides and/or oxy-hydroxide are also shown. Adding as little as 1 mol% Ga ion improved the 2-butanol total conversion by twice, and the MEK selectivity remarkably increased from 3 to 45%. The catalytic performance improved with the doping amount without changing the selectivity until 5 mol%. The selectivities, especially in the 1-butene/2-butenes ratio, gradually changed at a doping amount higher than 10 mol%. The gallium oxides and oxyhydride themselves were

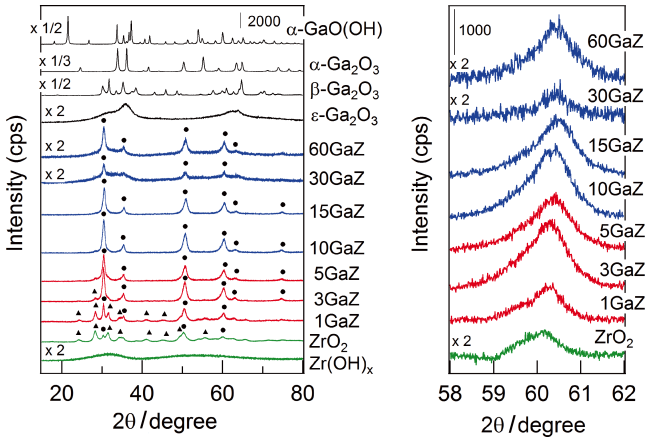

Fig. 3 XRD patterns of the Ga–ZrO_2 catalysts and reference compounds. ▲: Monoclinic-ZrO_2. ●: Tetragonal- and/or cubic-ZrO_2.

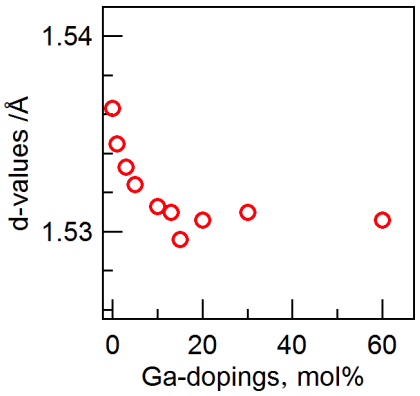

Fig. 4 Effect of gallium ion doping on the *d*-values for the tetragonal (211) or cubic (311) plane of ZrO_2.

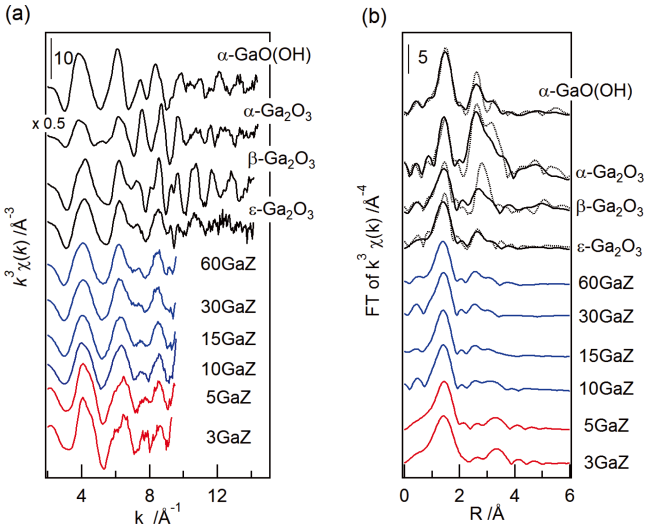

Fig. 5 Ga K-edge EXAFS spectra (a) and their Fourier transforms (b). Fourier range: *ca.* Δ*k*: 2.5 – 9.5 $Å^{-1}$ (dotted curves: *ca.* Δ*k*: 2.5 – 14.0 $Å^{-1}$).

more active for the 2-butanol conversion compared to Ga–ZrO_2. The MEK selectivities were *ca.* 30%, and 2-butenes were the main products.

XRD

Figure 3 shows the XRD patterns of the Ga–ZrO_2 catalysts and reference gallium compounds. The zirconium hydroxide precursor gave a typical halo pattern because of an amorphous phase. The 773 K calcination of the hydroxide resulted in the formation of a monoclinic- and tetragonal/cubic phase ZrO_2 mixture. The addition of Ga into ZrO_2 decreased the intensities of the diffraction lines because of the monoclinic ZrO_2 phase, but increased those of the tetragonal and/or cubic ZrO_2 phase, similar to that of a previous publication.[34] The diffraction lines due to crystalline ZrO_2 phases were weak for 30GaZ (30Ga–ZrO_2) and 60GaZ, which were overlapping with a broad band around 30 – 40°. The diffraction line around 60° shifted to a higher angle with the increasing doping amounts. Figure 4 shows the lattice spacing. The values decreased with the doping concentration until 10 mol%, and were constant in cases where the doped amounts were more than 10 mol%.

The present catalysts were prepared by calcination of a Ga ion-impregnated $Zr(OH)_x$ at 773 K for 3 h. Such a low calcination temperature was not enough to form highly crystallized ZrO_2 polymorphs, resulting in the identification of the crystalline phase (*i.e.*, whether tetragonal or cubic) to become difficult through XRD patterns recorded with a conventional diffractometer. In other words, the wide width of the diffraction line around 60° in the present XRD pattern made it difficult to assign whether the (211) plane of the tetragonal ZrO_2 or the (311) plane of the cubic phase.

EXAFS

Figure 5 shows the Ga K-edge EXAFS spectra of the Ga–ZrO_2 (GaZ) and Ga_2O_3 samples, and their radial structure functions (RSFs). The RSFs of all the GaZ samples possessed a large peak around 1.4 Å. A small peak was also observed around 3.3 Å for 3GaZ and 5GaZ as for the second coordination sphere. The spectral configurations of the RSFs of 30GaZ and 60GaZ were similar to those of ε-Ga_2O_3, and have a small peak around 3.5 Å. Table 1 summarizes results of the curve fitting analyses. The curve fitting analyses for a peak around 3 – 4 Å in the RSFs suggested that the second peak of low-doped catalysts, such as 3GaZ and 5GaZ were due to the Ga–Zr pair, whereas those of high-doped catalysts, such as 30GaZ and 60GaZ were due to the Ga–Ga pair.

Similar to the commonly available zirconium reagents, zirconium oxychloride used for the present starting material contained certain amounts of Hf. The available Ga K-edge EXAFS spectra of the GaZ samples were restricted up to *ca.* 9.4 $Å^{-1}$ because of the Hf L2 edge interference. The crystallographic data[23,35] of the Ga_2O_3 polymorphs showed that β-Ga_2O_3 and ε-Ga_2O_3 consist of GaO_6 and GaO_4 polyhedral units possessing both short (*ca.* 1.8 Å) and long Ga–O (*ca.* 2.0 Å) bondings. The α-Ga_2O_3 consists of the GaO_6 octahedra, but the Ga–O lengths are not uniform (1.921 and 2.077 Å).[36] Unfortunately, the available Δ*k* ranges of the present EXAFS spectra were as short as *ca.* 7 $Å^{-1}$. All analyses were conducted by a single-shell fitting of each coordination sphere to avoid lowering the analytical accuracy.

XANES

Figure 6 shows the Ga K-edge XANES spectra of GaZ and the reference compounds. All spectra gave an intense peak around 10374 eV. The spectral configuration gradually changed with the doping amount. A series of XANES spectra of GaZ samples had isosbestic points around 10377, 10383 and 10391 eV.

Table 1 Curve fitting analysis for the Ga K-edge EXAFS

Catalyst	SA[a]/ $m^2 \cdot g^{-1}$	Ga–O			Ga–Zr			Ga–Ga		
		CN[b]	r[c]/Å	$\Delta\sigma$[d]/Å	CN[b]	r[c]/Å	$\Delta\sigma$[d]/Å	CN[b]	r[c]/Å	$\Delta\sigma$[d]/Å
1GaZ	79									
3GaZ	62	8.0(1.5)	1.89(0.02)	0.125(0.028)	6.1(1.6)	3.57(0.01)	0.116(0.023)			
5GaZ	65	6.9(1.2)	1.89(0.02)	0.115(0.026)	2.8(0.8)	3.58(0.02)	0.089(0.029)			
10GaZ	60	6.4(1.1)	1.89(0.02)	0.109(0.026)	1.5(1.0)	3.54(0.04)	0.072(0.092)	1.0(1.1)	2.94(0.08)	0.104(0.117)
15GaZ	72	5.9(1.0)	1.89(0.02)	0.108(0.025)				1.0(0.3)	2.96(0.02)	0.073(0.034)
30GaZ	110	5.7(0.9)	1.89(0.02)	0.109(0.024)				1.5(0.4)	2.96(0.02)	0.096(0.027)
60GaZ	104	6.1(1.0)	1.89(0.02)	0.114(0.024)				2.6(0.7)	2.97(0.02)	0.108(0.023)
α-GaO(OH)	2.7[e]	7.8(1.2)	1.96(0.02)	0.105(0.025)				5.1(1.4)	2.98(0.02)	0.105(0.025)
α-Ga_2O_3	23	5.9(0.9)	1.93(0.01)	0.093(0.026)				5.5(1.8)	2.95(0.02)	0.062(0.046)
β-Ga_2O_3	19	6.7(1.1)	1.89(0.02)	0.120(0.025)				2.3(0.8)	3.04(0.02)	0.062(0.052)
ε-Ga_2O_3	88	6.4(1.1)	1.89(0.02)	0.116(0.026)				4.2(1.0)	2.99(0.02)	0.119(0.021)
ZrO_2	98									
Zr(OH)x	292[e]									

a. BET specific surface area. b. Coordination number. c. Interatomic distance. d. Debye–Waller factor. e. Outgassed at room temperature. Values in parentheses denote standard deviations.

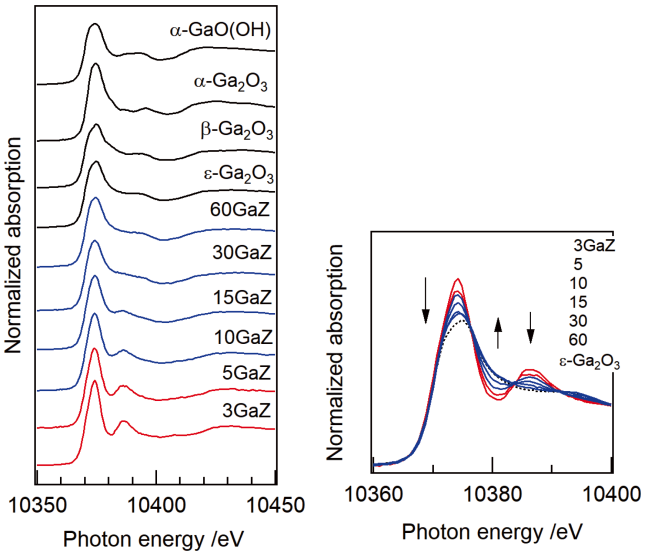

Fig. 6 Ga K-edge XANES spectra of the Ga-ZrO_2 catalysts and the reference compounds.

Discussion

Surface property

The catalytic performance of a secondary alcohol has been utilized for one of the test reactions to investigate the acid-base property of a catalyst.[2] In the case of the 2-butanol conversion, it has been recognized that acid and base sites promote dehydration to produce 2-butenes and dehydrogenation to produce MEK, respectively. In case both acid and base sites concertedly participate in this reaction, the α-olefin (1-butene) formation by the $E1_{cB}$ mechanism would be promoted.[2,6,37] The first step of 2-butanol dehydration *via* the $E1_{cB}$ mechanism is recognized as the formation of a carbanion where the basic site subtracts H^+ from C–H bond in the terminal methyl group. Similar to that in a previous publication,[38–41] the present ZrO_2 without addition of any metal cations promoted dehydration to preferentially produce 1-butene. The addition of the present Group 2 and 3 elements used in herein only little affected the catalytic performance of ZrO_2 itself, clearly showing that the surface acid-base property was not influenced by the addition of the elements utilized at the present reaction conditions. In contrast, Ga–ZrO_2 and In–ZrO_2 gave MEK as the main product. The product distributions (selectivities) for the Ga–ZrO_2 catalysts were almost identical to each other in cases where the doped amounts were 1 – 5 mol%, and were gradually approaching those of Ga_2O_3 with the loading amount. The GaZ catalysts could then be classified into two groups in terms of product distributions.

The MEK formation from 2-butanol might suggest that the present catalysts acted as a solid base such as MgO and CaO. Note that the catalytic dehydrogenation of hydrocarbons, such as propane and ethylbenzene, over supported and/or incorporated gallium oxide catalysts has been reported.[34,42–46] We then presumed the other possibility that the present Ga–ZrO_2 acted as a simple dehydrogenation catalyst of 2-butanol caused by Ga doping, independent of the solid basicity of a surface. This discussion is taken up in the following examination.

Strucural analysis

The ionic radius of Ga^{3+} is smaller than that of Zr^{4+} compared with the same coordination number (0.62 and 0.72 Å; *e.g.*, six-fold coordination[47]). A lattice constant of the crystalline ZrO_2 would then be decreased by Ga^{3+} doping if the $Ga_xZr_{1-x}O_2$ solid solution formed. The *d*-values for a peak around 60° decreased with the increase of the doping amount until 10 mol% (Figs. 2 and 3). In addition, the Fourier transformation of the Ga K-edge EXAFS spectra of GaZ showed that the peak position for the second coordination sphere in the RSFs around 3 – 4 Å differed by the doped amount. The curve fitting analyses suggested that the peak was due to Ga–(O)–Zr for 3 – 5 GaZ. The peak was confirmed to be Ga–(O)–Ga pairs for 30 – 60 Ga–ZrO_2. The shift of the *d*-spacing of a diffraction line around 60° and the curve fitting analyses clearly show that the $Ga_xZr_{1-x}O_2$ solid solution mainly formed for the low-doped Ga–ZrO_2, and the excess-doped Ga species existed as aggregates outside the solid solution for the high-doped Ga–ZrO_2. The EXAFS spectrum configuration of 60 GaZ resembled that of ε-Ga_2O_3 among those of the gallium oxide polymorphs. Only ε-Ga_2O_3 did not give intense diffraction lines in XRD patterns among the gallium oxide polymorphs utilized. The aggregated species

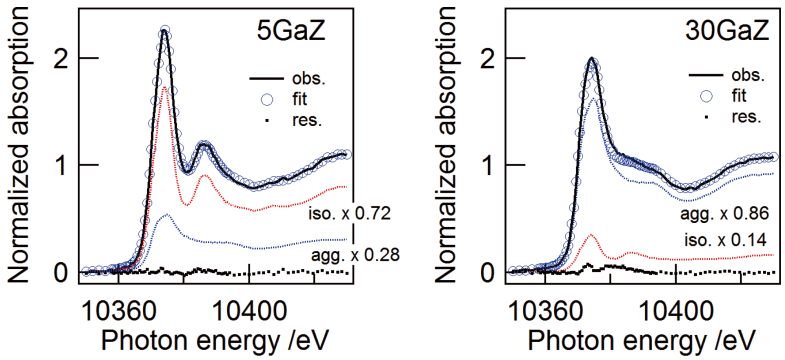

Fig. 7 Quantitative component analysis for the Ga K-edge XANES spectra of Ga-ZrO_2 with the isolated Ga species in ZrO_2 and the aggregated species (ε-Ga_2O_3).

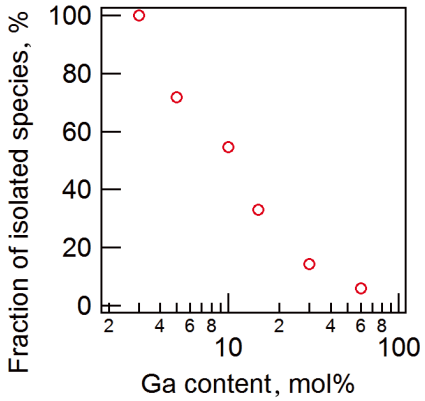

Fig. 8 Estimated fraction of the isolated Ga species forming the $Ga_xZr_{1-x}O_2$ solid solution in the Ga-ZrO_2 catalyst with different doping amounts.

were then presumably mainly ε-Ga_2O_3.

A series of XANES spectra possessed some isosbestic points as shown in Fig. 6. It suggests that two kinds of Ga species existed in a series of Ga-ZrO_2 catalysts, and the quantitative component analysis would be possible. We presume one is the ε-Ga_2O_3-like aggregated species, and the other is the $Ga_xZr_{1-x}O_2$ solid solution, where the Ga ions are atomically dispersed inside the bulk of ZrO_2. As for the standard spectrum for the solid solution, that of 3GaZ was adopted. The convolution analysis could successfully be carried out for all spectra. Figure 7 shows the typical results. Finally, the net Ga content in the $Ga_xZr_{1-x}O_2$ solid solution was evaluated by multiplying the Ga/(Ga + Zr) atomic ratio of Ga-ZrO_2 and the fraction of the isolated species. The x values for 5 – 60 GaZ were estimated as 0.035 – 0.055 (Fig. 8), showing that the upper solid solution limit was *ca.* 5 mol%, and the addition of 10 mol% Ga ion was required to form the saturated $Ga_xZr_{1-x}O_2$ solid solution.

Active species

As discussed above, two kinds of Ga-related species were suggested to exist in a series of Ga-ZrO_2 catalysts. One is the atomically dispersed species in Ga-ZrO_2 obtained by forming a solid solution (species A), and the other is the ε-Ga_2O_3-like aggregated species (species B). Species A existed as a main component in 1 – 5 GaZ, acted as an active site for selective dehydrogenation, and promoted the 2-butanol decomposition with the selectivity 46/41/10 for MEK/1-butene/2-butenes. A fraction of species B increased with the doping amount of Ga, resulting in the product selectivity gradually changing to that of species B itself. The temperature-programmed desorption experiments by the other research group revealed that various kinds of Ga_2O_3 polymorphs possessed both acid and base sites, and the amount of acid site was 10 times more than that of the base site.[29] The 2-butenes formation over Ga_2O_3 could then be promoted by the acidic site *via* the dehydration of 2-butanol according to Saytzeff's rule. Reasonably, the catalytic property of species B was similar to that of ε-Ga_2O_3. The catalytic performance, XANES/EXAFS, and XRD characterization support this deduction.

Acknowledgements

This work was partially supported by Japan Society for the Promotion of Science (JSPS) KAKENHI Grant Nos. 25630369 and 19K05150.

References

1. K. Tanabe, *Mater. Chem. Phys.*, **1985**, *13*, 347.
2. K. Tanabe, M. Misono, Y. Ono, and H. Hattori, "*New Solid Acids and Bases*", **1989**, Kodansha, Tokyo.
3. T. Yamaguchi, *Catal. Today*, **1994**, *20*, 199.
4. E. Iglesia, D. G. Barton, J. A. Biscardi, M. J. L. Gines, and S. L. Soled, *Catal. Today*, **1997**, *38*, 339.
5. Y. Ono and H. Hattori, "*Solid Base Catalysis*", **2011**, Tokyo Institute of Technology Press, Berlin.
6. H. Hattori and Y. Ono, "*Solid Acid Catalysis*", **2015**, Pan Stanford, Singapore.
7. M. Ozawa, M. Kimura, and A. Isogai, *J. Alloys Compd.*, **1993**, *193*, 73.
8. C. E. Hori, H. Permana, K. Y. S. Ng, A. Brenner, K. More, K. M. Rahmoeller, and D. Belton, *Appl. Catal. B*, **1998**, *16*, 105.
9. T. H. Etsell and S. N. Flengas, *Chem. Rev.*, **1970**, *70*, 339.
10. S. P. S. Badwal, *Solid State Ionics*, **1992**, *52*, 23.
11. M. Yashima, M. Kakihana, and M. Yoshimura, *Solid State Ionics*, **1996**, *86–88*, 1131.
12. K. Harada, H. Yamada, K. Okamoto, and A. Takami, *Catal. Surv. Asia*, **2010**, *14*, 176.
13. M. Hino and K. Arata, *J. Chem. Soc., Chem. Commun.*, **1988**, 1259.
14. K. Arata, *Appl. Catal. A*, **1996**, *146*, 3.

15. B. M. Reddy and A. Khan, *Catal. Rev. Sci. Eng.*, **2005**, *47*, 257.
16. T. Yamamoto, A. Orita, and T. Tanaka, *X-Ray Spectrom.*, **2008**, *37*, 226.
17. T. Yamamoto, *J. Jpn. Pet. Inst.*, **2014**, *57*, 261.
18. E. Iglesia, D. G. Barton, S. L. Soled, S. Miseo, J. E. Baumgartner, W. E. Gates, G. A. Fuentes, and G. D. Meitzner, *Stud. Surf. Sci. Catal.*, **1996**, *101A*, 533.
19. D. G. Barton, S. L. Soled, G. D. Meitzner, G. A. Fuentes, and E. Iglesia, *J. Catal.*, **1999**, *181*, 57.
20. T. Yamamoto, A. Teramachi, A. Orita, A. Kurimoto, T. Motoi, and T. Tanaka, *J. Phys. Chem. C*, **2016**, *120*, 19705.
21. T. Yamamoto, M. Kondo, T. Irie, and N. Tanima, *Adv. X-ray Chem. Anal. Jpn.*, **2017**, *48*, 137.
22. R. Roy, V. G. Hill, and E. F. Osborn, *J. Am. Chem. Soc.*, **1952**, *74*, 719.
23. H. Y. Playford, A. C. Hannon, E. R. Barney, and R. I. Walton, *Chem. Eur. J.*, **2013**, *19*, 2803.
24. T. Taguchi, J. Harada, A. Kiku, K. Tohji, and K. Shinoda, *J. Synchrotron Radiat.*, **2001**, *8*, 363.
25. T. Taguchi, T. Ozawa, and H. Yashiro, *Phys. Scr.*, **2005**, *T115*, 205.
26. T. Yamamoto, S. Mori, T. Kawaguchi, T. Tanaka, K. Nakanishi, T. Ohta, and J. Kawai, *J. Phys. Chem. C*, **2008**, *112*, 328.
27. T. Tanaka, H. Yamashita, R. Tsuchitani, T. Funabiki, and S. Yoshida, *J. Chem. Soc., Faraday Trans. 1*, **1988**, *84*, 2987.
28. A. L. Ankudinov, B. Ravel, J. J. Rehr, and S. D. Conradson, *Phys. Rev. B*, **1998**, *58*, 7565.
29. B. Zheng, W. Hua, Y. Yue, and Z. Gao, *J. Catal.*, **2005**, *232*, 143.
30. W. Jochum, S. Penner, K. Föttinger, R. Kramer, G. Rupprechter, and B. Klötzer, *J. Catal.*, **2008**, *256*, 268.
31. L. Li, W. Wei, and M. Behrens, *Solid State Sci.*, **2012**, *14*, 971.
32. P. W. Park, C. S. Ragle, C. L. Boyer, M. L. Balmer, M. Engelhard, and D. McCready, *J. Catal.*, **2002**, *210*, 97.
33. M. Chen, J. Xu, Y. Cao, H. Y. He, K. N. Fan, and J. H. Zhuang, *J. Catal.*, **2010**, *272*, 101.
34. H. Li, Y. Yue, C. Miao, Z. Xie, W. Hua, and Z. Gao, *Catal. Commun.*, **2007**, *8*, 1317.
35. J. Åhman, G. Svensson, and J. Albertsson, *Acta Crystallogr., Sect. C*, **1996**, *52*, 1336.
36. M. Marezio and J. P. Remeika, *J. Chem. Phys.*, **1967**, *46*, 1862.
37. K. Thomke, *Proc. 6th. Int. Congr. Catal.*, **1977**, *I*, 303.
38. T. Yamaguchi, H. Sasaki, and K. Tanabe, *Chem. Lett.*, **1973**, *2*, 1017.
39. B. H. Davis and P. Ganesan, *Ind. Eng. Chem. Prod. Res. Dev.*, **1979**, *18*, 191.
40. A. Auroux, P. Artizzu, I. Ferino, V. Solinas, G. Leofanti, M. Padovan, G. Messina, and R. Mansani, *J. Chem. Soc., Faraday Trans.*, **1995**, *91*, 3263.
41. T. Yamamoto, T. Tanaka, T. Matsuyama, T. Funabiki, and S. Yoshida, *J. Phys. Chem. B*, **2001**, *105*, 1908.
42. H. Kitagawa, Y. Sendoda, and Y. Ono, *J. Catal.*, **1986**, *101*, 12.
43. N. S. Gnep, J. Y. Doyement, and M. Guisnet, *J. Mol. Catal.*, **1988**, *45*, 281.
44. K. Nakagawa, M. Okamura, N. Ikenaga, T. Suzuki, and T. Kobayashi, *Chem. Commun.*, **1998**, 1025.
45. J. N. Park, J. Noh, J. S. Chang, and S. E. Park, *Catal. Lett.*, **2000**, *65*, 75.
46. M. Chen, J. Xu, F. Z. Su, Y. M. Liu, Y. Cao, H. Y. He, and K. N. Fan, *J. Catal.*, **2008**, *256*, 293.
47. R. D. Shannon, *Acta Crystallogr., Sect. A*, **1976**, *32*, 751.